We thank both reviewers for their careful reading of the manuscript and their insightful comments, which have encouraged us to make revisions that have significantly strengthened the analysis. We provide a detailed response to their comments below, with the original comments from the reviewers in **black**, our responses in **blue**, and changes to the manuscript in **green**. Line numbers correspond to the revised manuscript. Based on the reviewers' comments, we have made the following major changes to our analysis and the manuscript:

1) We updated the discussion and analysis of the latent space representations to provide more connection between the learned latent variables and typical signal analysis methods.
2) We have added a comparison between the VAE analysis and a PCA analysis to demonstrate the potential value added by the non-linear dimensionality reduction method
3) We have replaced the section on outlier detection with a section on using cosine similarity as a metric to compare the within-class and between-class similarity of L-II signals.

We have also updated the github repository so that our analysis can now be easily reproduced using Google Colab.

****

Reviewer 2:

This study presents a new method for classifying aerosol particles based on the Laser-Induced Incandescence (L-II) signals using unsupervised machine learning. The author applied Variational Autoencoder (VAE) to analyze L-II signals and compress into a lower-dimensional latent space. This approach is an improvement because it removes the need for manual feature engineering. The paper is well-structured and easy to follow. The introduction provides sufficient background on the SP2 and the limitations of previous classifying methods. The methods section clearly describes the dataset, data preprocessing, and the VAE model. Despite these strengths, there are several issues that must be addressed before publication.

We thank the reviewer for their thoughtful comments, and their positive feedback.

General comments:

1. **Physical Interpretation of Latent Space:** While the VAE approach is a powerful tool for classifying aerosol types, the discussion on the physical interpretation of the latent space (e.g., z1−z4) feels underdeveloped. The connection between the latent representation and blackbody temperature (Figure 3) is fascinating and a key finding. What specific features of the L-II signals (e.g., peak sharpness, symmetry, or decay rate) are being captured by these latent variables? A more thorough discussion linking the distributions in Figures 5

and 6 to the microphysical properties of the different aerosol types (BC, FeOx, dust) would significantly strengthen the paper's scientific contribution.

We have now included additional analysis of the decoded signals from the latent space manifolds, which demonstrate what specific types of variability are being picked up by the variational autoencoder in Figure 7, shown below.

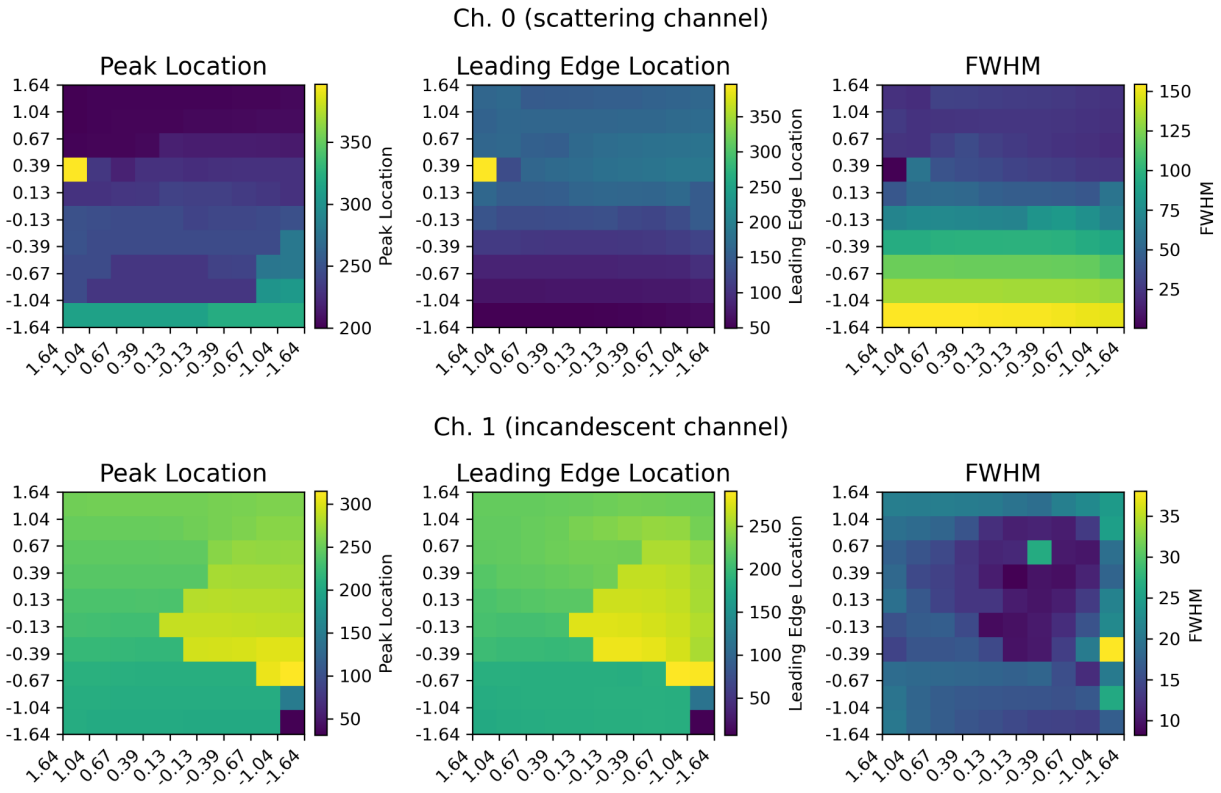

Figure 7: Signal Analysis of Latent Manifolds for the L-II Signals. The main peak location, peak leading edge location (defined as the leading edge of the largest peak at half maximum), and full-width half maximum for the decoded L-II signals for Ch. 0 (top row) and Ch. 1 (bottom row). The peak location, leading edge location, and FWHM width are all given in terms of digitalized time points (out of 400 for the NOAA SP2).

We have added the following discussion to the manuscript in lines 293 - 301:

To more quantitatively assess the types of variability learned by the VAEs for Ch. 0 and Ch. 1, we analyze the decoded signals associated with each decile, using the scipy package (Virtanen et al. 202). We use the find_peaks function in scipy to find the largest peak in each time series, and then determine the peak location (in terms of digitized time points). We also use the peak_widths function to determine the width of the full width half maximum (FWHM) of this peak, as well as

the digitized time point of the leading edge of the peak at half maximum (which we refer to as leading edge location). The values associated with the decoded signals of the latent manifolds for both Ch. 0 and Ch. 1 are shown in Figure 7. For Ch. 0 in particular it is clear that both the leading edge location and the FWHM are strongly correlated with z_2. For Ch. 1, the peak location and leading edge location have their highest values (associated with later times in the L-II signals) towards the center of the manifold. The signals at the center of the manifold are also associated with more narrow peaks in terms of their FWHM.

2. **Outlier Detection and Ambient Data:** The claim that outlier detection can be useful for characterizing aerosols from various sources (Lines 293-301) seems a strong assertion. While this is a promising application, the current study, which uses laboratory-generated data, does not provide sufficient evidence to support this claim for ambient atmospheric observations. To make this point more convincing, the authors would need to analyze real atmospheric data. I recommend toning down this claim to a more cautious statement about the potential for this method to be applied to ambient data in future work.

We have now replaced the section on outlier detection to include a calculation of the cosine similarity between the different embedding the signal (2D VAE, 3D VAE, and PCA) in order to demonstrate which classes show the most similarity to one another in Figure 8. We have updated the discussion to suggest that outlier detection will be a promising future direction of research in using unsupervised machine learning for analysis of the L-II signals from the SP2.

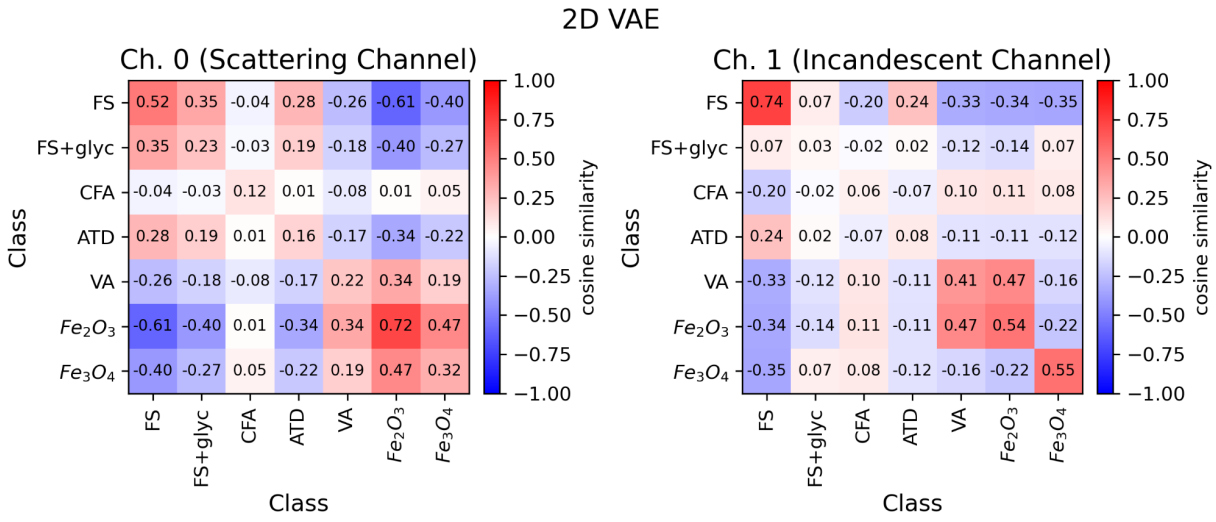

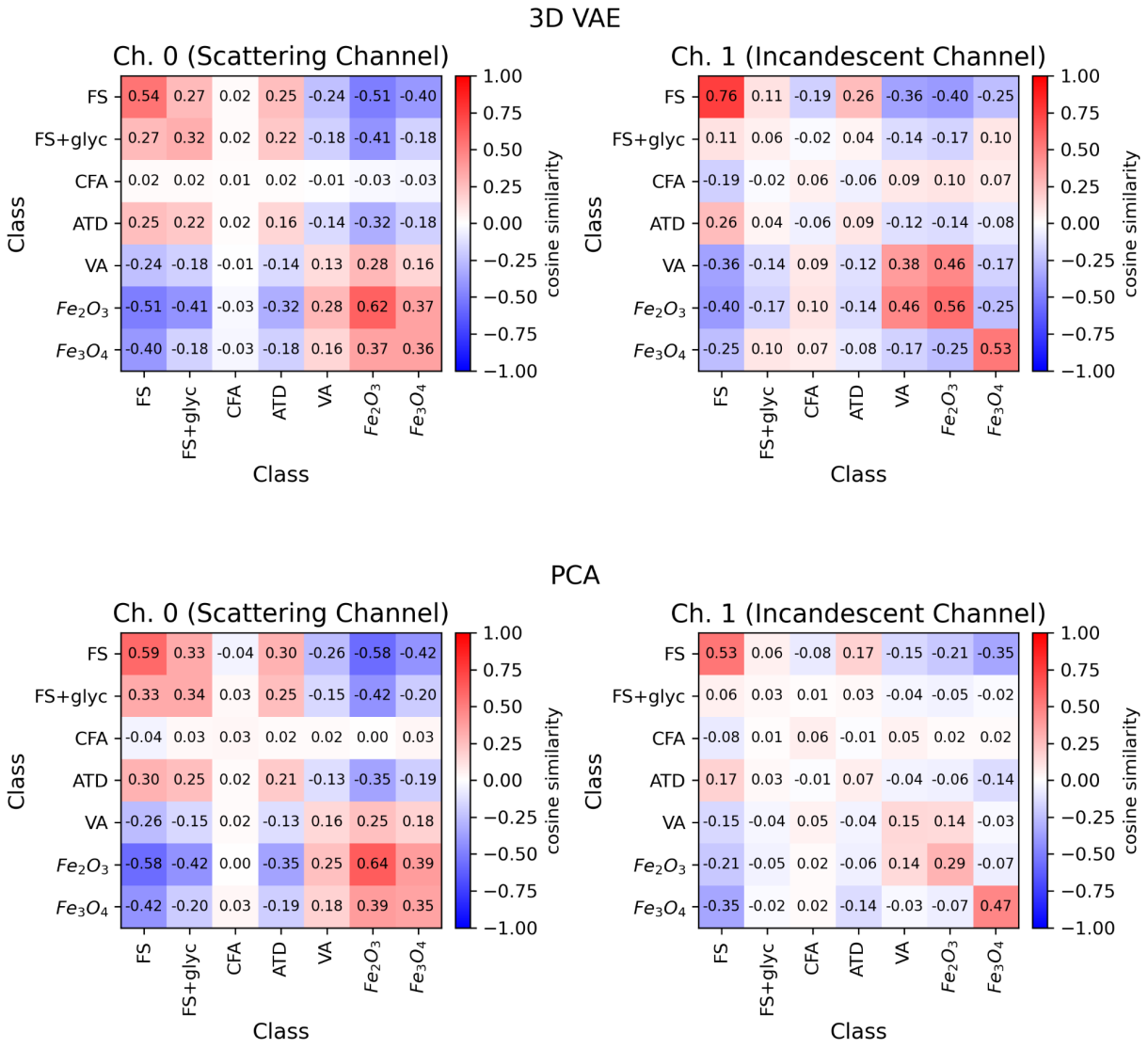

3. **Figure Readability:** Overall, the font size for text within the figures, including labels and legends, is too small and difficult to read. The marker sizes in the legends are also unclear, making it hard to distinguish between different aerosol types. I would recommend that the authors increase the font size and marker size to improve the readability of all figures.

We have now updated the font size throughout the manuscript so that figures are more readable.

Specific comments:

1. Lines 29-30: Please re-check the citation for Moteki and Kondo (2010). This paper does not focus on a field study of rBC. The citation should be removed or replaced with a more relevant reference.

Thank you for pointing this out. We have replaced the citation with Moteki et al. 2014 instead.

Moteki, N., Y. Kondo, and K. Adachi (2014), Identification by single-particle soot photometer of black carbon particles attached to other particles: Laboratory experiments and ground observations in Tokyo, *J. Geophys. Res. Atmos.*, 119, 1031–1043, doi:10.1002/2013JD020655.

2. Line 78: The chemical formula of Iron (IV) should be corrected to Iron (II, III).

Thank you. Updated.

3. Line 131: The text should be corrected from Ch. 0 to Ch. 1.

Updated.

4. Figure 2: Please correct “Fe203” and “Fe3O4” to “Fe_2O_3” and “Fe_3O_4”. Additionally, please correct “Schwartz et. al 2006.”

We have updated the figure to fix the typos.

5. Figure 2: In the center upper panels, “Class 1” and “Class 2” are not defined. Could you clarify what these classes represent?

We have now added the class labels in Table 1.

6. Line 216: Please correct the spelling of “Fe*O*x”. I would recommend the thorough check of the entire manuscript.

We have checked the spelling throughout the manuscript.

7. Figure 4: Why are “z1” and “z3” denoted in x labels and “z2” and “z4” denoted in y labels? It seems that they should be “time” and “signal amplitude.”

Here we are denoting the direction of variability sampled for the latent manifold. By sampling along the deciles of the distributions of z1 and z2 variables (in the left panels) and the deciles of the distribution of z3 and z4 (in the right panel), we visualize characteristic L-II signals at each of those points (using the trained decoder to map back to the high dimensional time series space). We have now added the values of the latent variables that are decoded in each subplot along the x and y-axis so that this is clear.

To clarify this, we have updated the caption in (now) Figure 6 to read:

Latent Manifolds for the L-II Signals. By sampling along the deciles of a gaussian distribution for the 2 latent variables from each channel, we visualize characteristic L-II signals using the trained decoder. These learned latent manifolds provide an overview of the modes of variability described by the latent representations of the two channels. **Left: Latent Manifold for Channel 0, showing the variability represented by z1 (x-axis) and z2 (y-axis). Right: Latent Manifold for Channel 1, showing the variability represented by z3 (x-axis) and z4 (y-axis).**

8. Figure 4: The "Noise" signals are not explicitly defined. It would be helpful to provide a clear definition of "Noise" signal in this context.

Because the signals are normalized between 0 and 1, this part of the latent space for Ch. 0 appears to pick up relatively small scattering signals, where the noise on the baseline is comparable to the height of the peaks in the signal. We have added this point to the text in Lines 289-292:

Because the signals are normalized between 0 and 1, the top left part of the latent space for Ch. 0 appears to pick up relatively small scattering signals, where the noise on the baseline is comparable to the height of the peaks in the signal.

9. Lines 242–244 and Figure 5: The authors state that there is “significant overlap” between FS and FS+glyc. However, the distributions for Ch 1 (z4 vs z3) appear to be different.

This is a great point, and it is potentially due to differences in the thermal lensing between the coated and uncoated FS particles. While a significant portion of the latent space shows an overlap between the particles, there is also a population of FS+glyc signals that show up with high density in the top right part of the Ch. 1 latent space. We have added this point to the text in lines 306-310:

However, there are also regions of high density for the Ch. 1 embeddings of the FS+glyc samples that are not occupied by the FS samples. Similarly, for the two iron oxides, Fe_2O_3 has a higher density of points near the origin and for positive values of z_4 when compared to Fe_3O_4. This suggests that while there are some similarities between the latent embeddings for the two types of FS and for the two iron oxide aerosols, there are some notable differences in terms of their response in the SP2. We quantify this similarity further in Section 5.

10. Line 278: It seems that “outlier increases” should be corrected to “outlier decreases.”

Good point. Based on the major comments from both reviewers, we have chosen to focus on quantifying within-class and between-class similarity, and have removed the section on outlier detection.

11. Figure 7: The scatter plots of z4 and z3 in the left two panels appear to be almost identical. It would be more efficient to include only one panel. Additionally, please clarify what the dashed lines indicate and confirm that they correspond to the selected outlier markers.
12. Figure 7: The signals of Channel 3 are difficult to interpret for unfamiliar reader to interpret. It would be helpful that author to include an example of a normal signal of Channel 3 as well as Channels 0 and 1 showed in Figure 2.

We have now removed Figure 7 and replaced this outlier analysis with a comparison of the cosine similarity of the embeddings of the different aerosol classes.

13. Lines 281–285: Please provide a physical explanation for why these specific outliers occurred. For example, was the Fe_3O_4 outlier due to the multiple detection of particles?

For the Fe_3O_4 particle (top panel, right), this particle was likely considered an outlier because two particles passed through the beam during the same triggering window, which is evident in the inset plot for Ch. 0. For the CFA particle (bottom panel, right), this L-II signal was identified as an outlier because the particle was very large (clear from the saturated peak in Ch. 0 and the irregular signal in Ch. 4) and incandescent occurred relatively late during the time the particle was passing through ND:YAG laser beam (clear from the incandescence peaks in Ch. 1 and 2 being shifted to the far right in the time series signals).

As mentioned in the previous comments, we have chosen to remove the section on outlier detection and instead include a section on quantifying the variability in aerosol populations using their L-II embeddings.